PROGRESS IN COLOR, COLORANTS AND COATINGS

available online @ www.pccc.icrc.ac.ir

Progress in Color Colorants Coating 19 (2026), 363-373

Ministry of Science, Research and Technology
Institute for Color Science & Technology

A Dual-Functional Surfactant Strategy for High-Yield Synthesis of Epoxy-Loaded Melamine Formaldehyde Microcapsules

E. Babaei, M. Pishvaei*, F. Najafi
Department of Resin and Additives, Institute for Color Science and Technology, P.O. Box: 16765-654, Tehran, Iran

ARTICLE INFO

Article history:
Received: 08 Aug 2025
Final Revised: 26 Oct 2025
Accepted: 27 Oct 2025
Available online: 16 Feb 2026

Keywords:
Microcapsule
Encapsulation efficiency
Dual functional surfactant
Epoxy
Melamine formaldehyde

ABSTRACT

The encapsulation of various healing agents can be achieved using amino resins as the shell material. For optimal encapsulation efficiency, pH adjustment is a critical parameter. In this study, epoxy resin was encapsulated via in-situ interfacial polymerization in an oil-in-water emulsion. A dual-functional surfactant featuring a quaternary ammonium moiety serving as the hydrophilic head group, combined with precise pH control, was employed. In addition to catalyzing amino resin formation at the interface, this surfactant significantly suppresses the formation of unwanted nanoparticles. Furthermore, citric acid, used for pH adjustment, also acts as a surfactant due to its structural properties, preferentially localizing at the epoxy/water interface.As a result,a high encapsulation efficiency of 92 % isachieved,which displaysan improvement of about 25 % over conventional ammonium chloride-catalyzed methods. The core-to-wall ratio was systematically optimized, with a 1:2 ratio yielding the highest encapsulation efficiency (92 %), while a 1:3 ratio led to a 15 % efficiency drop. Furthermore, stirring rate modulation enabled size control, producing capsules ranging from 1 μm (at 1100 rpm) to 2 μm (at 500 rpm). Surfactant concentration critically influenced unwanted nano particle formation and encapsulation efficiency where, using 1 wt. % of surfactant, a 92 % encapsulation efficiency was achieved, while concentrations at 10 wt. % caused a 28 % efficiency decline due to excessive aqueous-phase polymerization and capsule aggregation. This work establishes a comprehensive framework for microcapsule synthesis, enablingthe design oftailored microcapsule for high-performance self-healing applications. Prog Color Colorants Coat. 19 (2026), 363-373© Institute for Color Science and Technology.

1. Introduction

Self-healing polymeric materials have drawn significant inspiration from biological systems capable of autonomous repair [1]. The field was fundamentally transformed by early work demonstrating micro-encapsulated dicyclopentadiene in poly(urea-formal-dehyde) shells [2], with subsequent studies identifying epoxy resins as superior healing agents due to their matrix compatibility [3]. However, three persistent challenges remain: suboptimal encapsulation efficiency (< 70 % in most systems) [4], unwanted nanoparticle formation [5], and premature epoxy ring-opening under acidic catalytic conditions [6, 7].

Recent developments have achieved partial solutions. Solvent-based systems showed economic viability but limited bonding [7], while isocyanate chemistry enabled moisture-triggered healing [8], though with sensitivity to environmental humidity [9].

*Corresponding author: * pishvaei@icrc.ac.ir
https://doi.org/10.30509/pccc.2025.167621.1428

Living polymerization techniques created covalent bonds in thermoplastics [9], though with restricted applicability to specific matrix compositions [10, 11]. pH-responsive systems achieved >90 % encapsulation at optimal pH [12]. Green chemistry approaches utilizing citric acidstrike a balance between efficiency and sustainability [13], in contrast microfluidic methods produce monodisperse capsules [14] but require complex equipment unsuitable for large-scale production [14]. Quaternary ammonium surfactants addressed interfacial stability [15], and core-shell optimization enhanced healing performance [16]. Despite these advances, previous methods often addressed these challengesseparately [17], with limited success in simultaneously preventing epoxy ring-opening while maintaining high encapsulation efficiency under acidic conditions [17, 18].

This work overcomes these limitations through a pH-stable encapsulation system that prevents epoxy degradation while enabling high-yield encapsulation. Our dual-functional surfactant strategy simultaneously catalyzes melamine-formaldehyde shell formation and maintains epoxy integrity, achieving 92 % encapsulation yield - surpassing the 70-88 % range reported in prior art [4, 7, 11]. Unlike microfluidic methods requiring complex equipment [14, 19-21], this system employs conventional stirring for scalable production. Our approach uniquely combines the interfacial activity of quaternary ammonium surfactants [15, 22] with the pH-modulating effect of citric acid [19, 23], creating an optimal environment for both encapsulation efficiency and epoxy stability [24]. This synergistic strategy represents a significant advancement over previous approaches that could not simultaneously resolve the conflict between catalytic efficiency and epoxy preservation [25-29].

2. Experimental

2.1. Materials

The chemicals used in this study included butyl 2,3-epoxypropyl ether, 2-ethylhexanol, melamine, citric acid, and formaldehyde, all obtained from Merck Chemicals. Diglycidyl ether of bisphenol A (DGEBA) was sourced from Epotech Chemicals, poly(vinyl alcohol) (PVA) from Air Products, and the cationic surfactant Siquat BAC 80 from Sichem Chemicals.

2.2. Preparation method

Microcapsules were prepared through an in-situ oil-in-water interfacial polymerization process. The synthesis began with the preparation of melamine-formaldehyde prepolymer, where 3.81 g of melamine reacted with 6.89 g of formaldehyde (37 wt. % aqueous solution) in 50 mL of distilled water within a three-neck flask. This mixture was heated at 70 °C for 25 minutes until a clear prepolymer solution formed, as illustrated schematically in Figure 1.

Concurrently, aqueous solutions of Siquat BAC 80 and PVA were prepared by heating and magnetic stirring. The core material, consisting of a 30:70 wt. % mixture of butyl 2,3-epoxypropyl ether and DGEBA, was then emulsified into the surfactant solution under continuous stirring for 30 minutes. The MF prepolymer solution was subsequently introduced to this emulsion to form melamine formaldehyde shell (Figure 2), so the reaction proceeded for 300 minutes at 75 °C under controlled pH and stirring conditions. Different samples with given parameters (Table 1) have been synthe-sized. Figure 3 shows schematically the microcapsules structure.

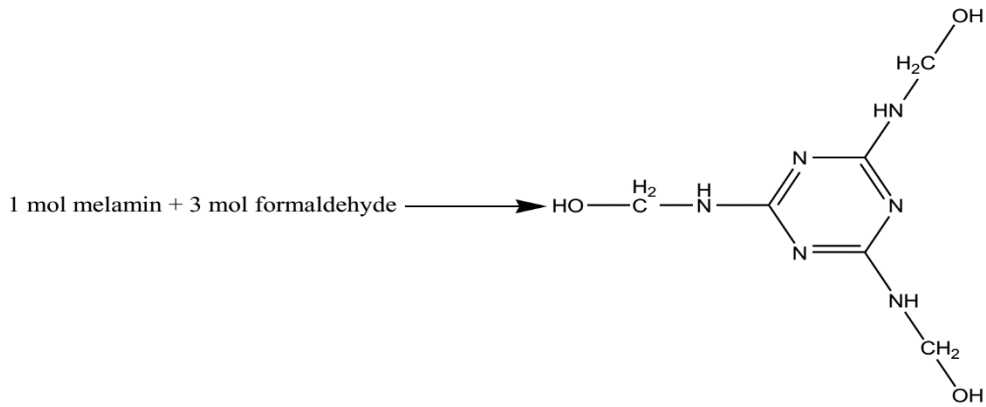

Figure 1: Schematic preparation of melamine formaldehyde pre polymer.

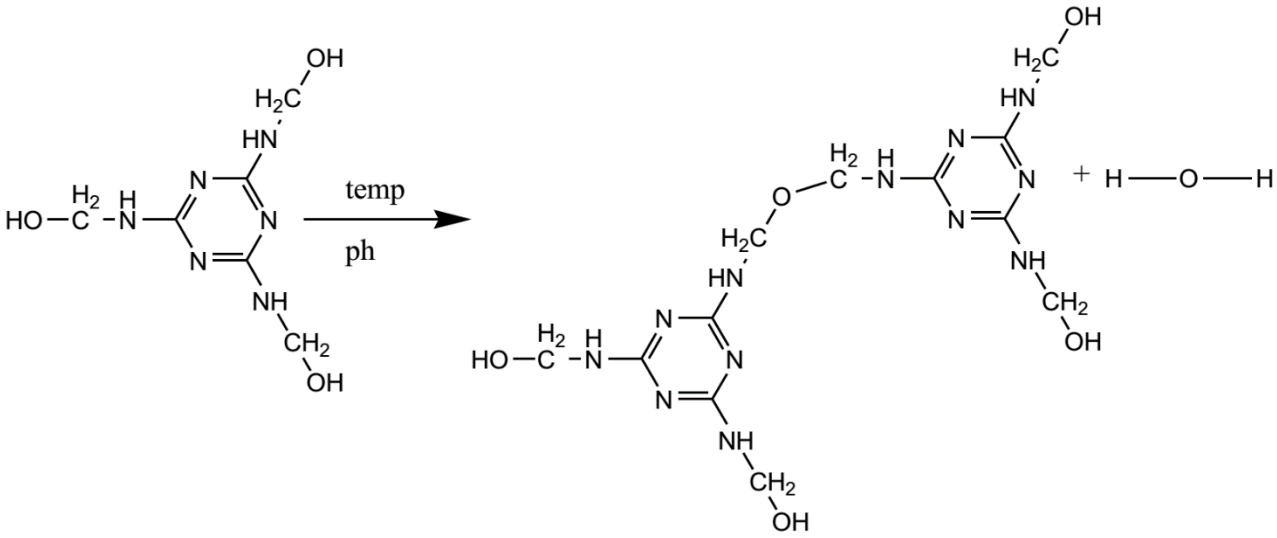

Figure 2: Schematic of melamine formaldehyde formation.

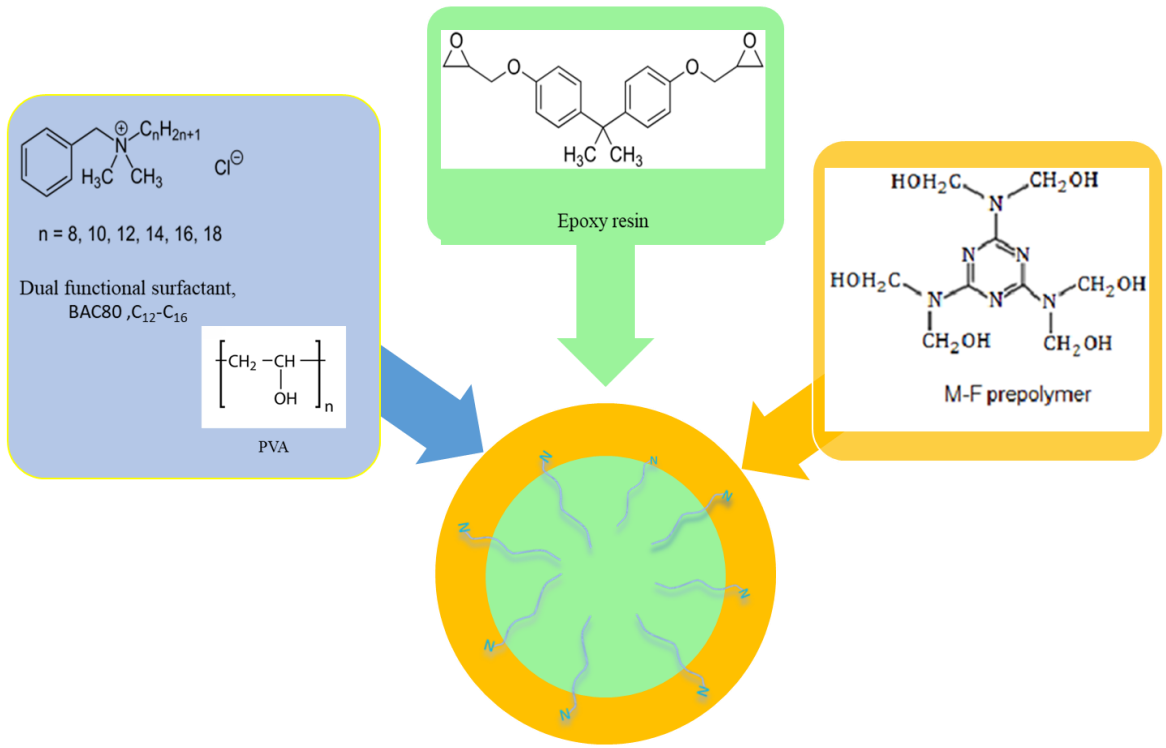

Figure 3: Schematic of microcapsule structure.

Table1: Different characters of experimental systems.

Sample name	Wall material	Core/wall	Siquat Bac 80 %	Stiring speed (rpm)	Efficiency % (Error ± 2%)	Average size* (µm)
Mc1	MUF	2	1	400	72.5	4
Mc2	MF	2	1	500	91.8	2
Mc3	MF	2	1	800	86.6	1.5
Mc4	MF	2	1	1100	81.5	1
Mc5	MF	4	1	500	23.09	1.5
Mc6	MF	3	1	500	78.3	2
Mc7	MF	2	10	1100	63.4	2.5
Mc8	MF	2	5	1100	73.2	2.5
Mc9	MF	2	5	1400	50.4	0.5 - 3
Mc10	MF	2	1	200	56.7	2.5
Mc11	MF	2	5	1100	65.4	4
Mc12	MF	2	1	500	86.1	2
Mc13	MF	2	5	800	68.6	3

*Based on SEM images

The resulting microcapsules were isolated by filtration, thoroughly washed with deionized water, and air-dried. Formation of microcapsules was initially verified through scanning electron microscopy (SEM), with subsequent confirmation of chemical composition by FT-IR spectroscopy. SEM analysis also provided measurements of capsule size distribution, while thermogravimetric analysis (TGA) characterized the microcapsules' core content, capsule-wall thickness, and thermal stability profiles.

2.3. Characterization methods:

The infrared spectra of the samples were recorded in the rangeof 4000 to 500 cm^{-1} on the ATR mode of the Fourier transform infrared spectrometer (FTIR Bruker, model: VERTEX 70). Thermogravimetric analysis (TG/DTA) was carried out onaPyrif diamond instrument (SII) (Perkin Elmer Ltd., US) under a nitrogen atmosphere. The rate of heating was 10 ^{o}C/min. The microstructure of the samples was examined using a scanningelectron microscope (SEM), LEO 1455VP. The samples were diluted with deionized water and dried on a cover glass before examination.

3. Result and Discussion

3.1. Encapsulation efficiency

The preparation yield was determined as the mass ratio of recovered microcapsules to the total mass of core and shell constituents [3]. To isolate the microcapsules, a rigorous washing protocol was employed: the slurry was repeatedly treated with acetone, followed by drying and weighing, until the mass of recovered capsules stabilized between two consecutive washing cycles. This ensured thecomplete removal of unencapsulated residues. The microencapsulation efficiency was then calculated using equation 1. Encapsulation efficiency is equal tothe Mass of recovered microcapsules (W_e) divided by Wp(Mass of core material + Mass of shell constituents).

$$\eta = W_e / W_p \times 100 \quad (1)$$

This methodology provided an accurate assessment of the encapsulation process effectiveness by accounting for both core retention and shell integrity. The iterative washing procedure eliminated potential overestimation caused by residual surfactants or unreacted monomers, in alignment with established purification practices in microcapsule synthesis [3, 7]. Notably, our protocol

improves upon conventional single-wash methods by verifying mass equilibrium, thereby enhancing reproducibility.

3.2. Capsule chemical structure

The FT-IR spectrum of sample Mc2 (Figure 4) exhibits characteristic absorption bands corresponding to key functional groups: the epoxy ring stretching vibration is observed at 1247 cm^{-1}, while aromatic C=C stretching is observed at 1590 cm^{-1}. Distinct melamine-formaldehyde vibration associated with melamine-formaldehyde shell is observedthrough the C=N melamine ring vibration at 1509 cm^{-1}, C-N linkage to the melamine ring at 1342 cm^{-1}, and C-N formaldehyde bonding at 1183 cm^{-1}. Most significantly, the simultaneous detection of epoxy ring vibrations and aromatic C=C stretching provides conclusive evidence for successful epoxy resin encapsulation within the microcapsules. These spectral features collectively verify three critical aspects of the microcapsule structure: intact melamine-formaldehyde shell formation, preservation of epoxy functional groups in the core material, and absence of significant side reactions during encapsulation.

3.3. Capsule diameter

Capsule diameter was precisely controlled by adjusting the stirring rate during synthesis. As demonstrated in Figure 5, increasing the stirring rate from 500 to 1100 rpm resulted in a systematic reduction in average capsule size from 2 μm to 1 μm (Mc2, Mc4). This inverse relationship follows the Kolmogorov-Hinze theory of droplet breakup, where capsule diameter (d) scales with stirring rate (N) as d ∝ N^(-0.6) under turbulent conditions [21]. The increased stirring rate not only reduced capsule dimensions but also enhanced size uniformity and improved sphericity, as evidenced by the narrower size distribution and more regular morphological features observed at elevated rotation speeds. This tunable control over capsule size while maintaining morphological integrity is particularly valuable for applications requiring precise regulation of release kinetics, such as self-healing coatings [1] or drug delivery systems [21].

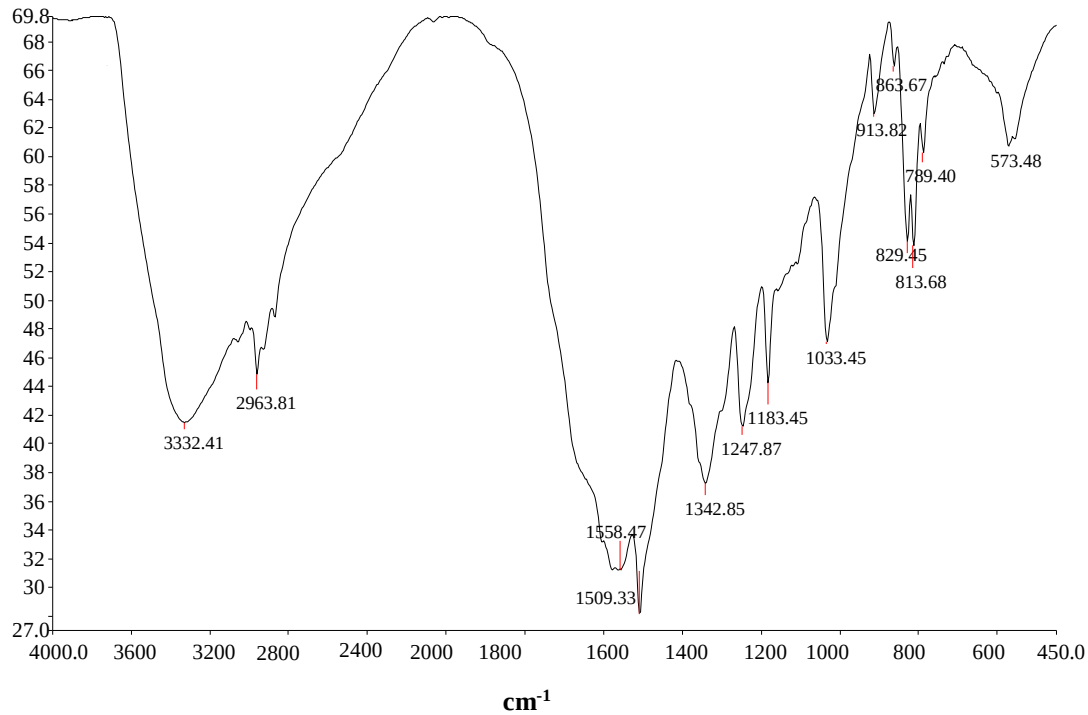

Figure 4: Fourier transform infrared spectroscopy analysis of Mc2 sample.

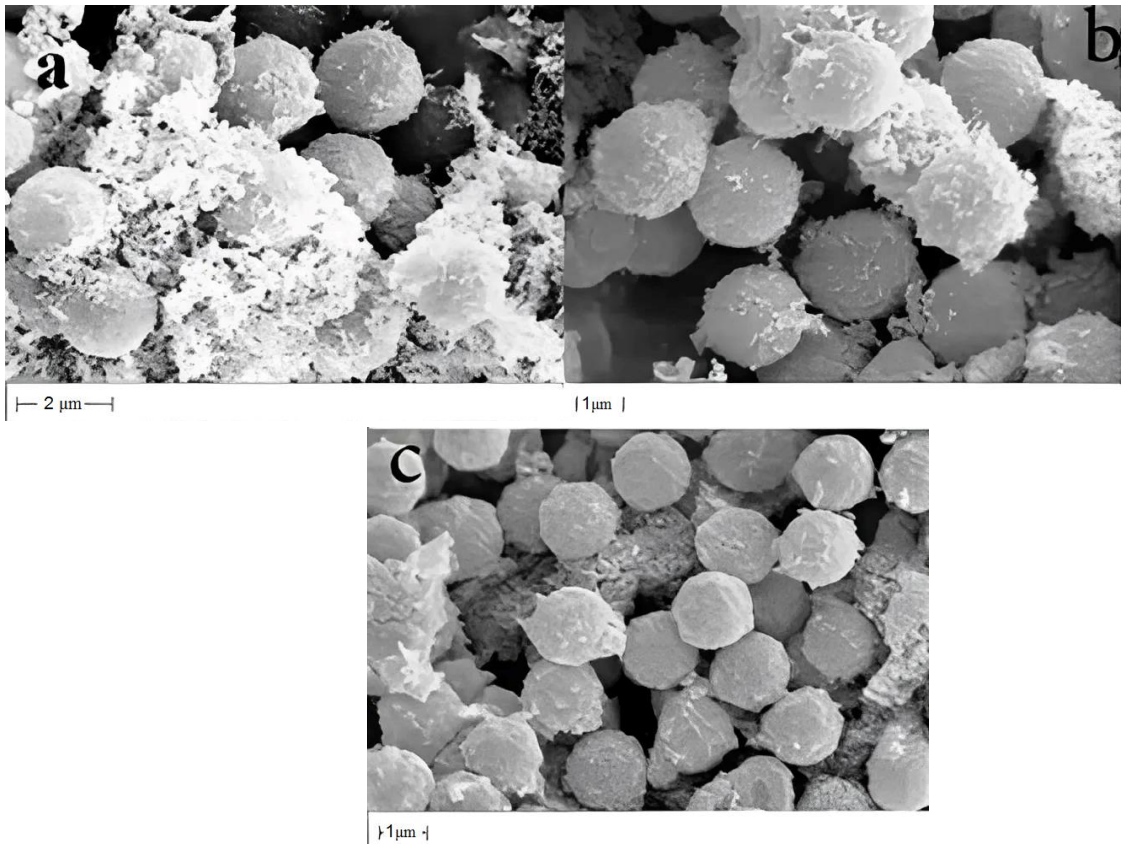

Figure 5: SEM images of samples at different stirring rate a) 500 rpm, b) 800rpm and c) 1100 rpm.

The inverse relationship between capsule size and surface-area-to-volume ratio (SA/V ∝ 1/r) fundamentally governs shell material requirements during microencapsulation. As capsule size decreases with higher stirring rates, the increased total surface area requires proportionally more shell material to maintain complete coverage. This geometric constraint explains the observed reduction in residual melamine formaldehyde nanoparticles; available precursors are preferentially consumed for interfacial polymerization rather than forming discrete nanoparticles [22]. However, as shown in Figure 6, excessive shear rates (≥1100 rpm) induce mechanical fracture of micro-capsules during formation, compromising encap-sulation efficiency as observed by Brown et al [3]. These competing effects demonstrate the need for balanced process optimization between capsule size reduction and structural preservation.

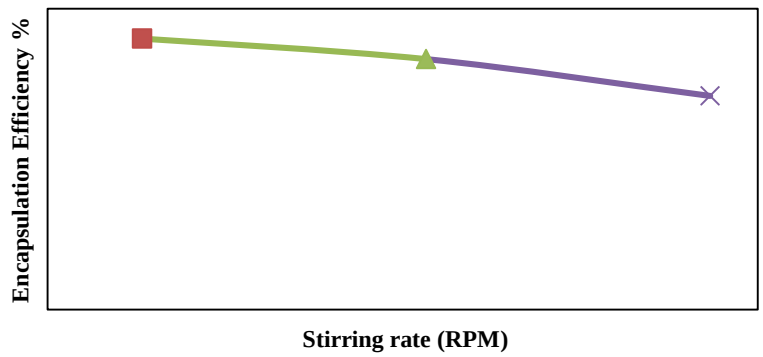

Figure 6: Encapsulation efficiency vs. stirring rate.

3.4. Capsule shell thickness

Shell thickness was rigorously evaluated through complementary thermogravimetric analysis (TGA), with validation via scanning electron microscopy (SEM) where feasible. While SEM theoretically enables direct thickness measurement through cross-sectional imaging, practical limitations arise when analyzing micron-scale capsules: (1) Mechanical sectioning often damages fragile shells, distorting measurements; (2) The spherical geometry introduces parallax errors in 2D imaging; and (3) Representative sampling requires statistically significant particle counts (>100 capsules) for reliable averaging [23].

The residual weight at 600 °C in TGA curves directly correlates with the microcapsule shell content of the particles with the same diameter, where a reduction in residual weight indicates thinner shell walls. To systematically control the shell thickness, the initial core-to-wall ratio was increased from 2:1 to 3:1. The results (Figures 7 and 8) demonstrate an inverse relationship between core-to-wall ratio and shell thickness, where experimental values closely approximate theoretical predictions. The thermal decomposition profile reveals three characteristic events: an initial weight loss near 100 °C corresponding to volatilization of butyl 2,3-epoxypropyl ether used as epoxy diluent, followed by a 200 °C transition attributed to deformaldehydation of the melamine-formaldehyde shell matrix. The primary decomposition event at 400 °C reflects thermal degradation of the encapsulated epoxy resin core. The final residual weight percentage provides a quantitative measure of the shell material content, confirming that increased core-to-wall ratios effectively produce microcapsules with proportionally thinner walls while maintaining structural integrity.

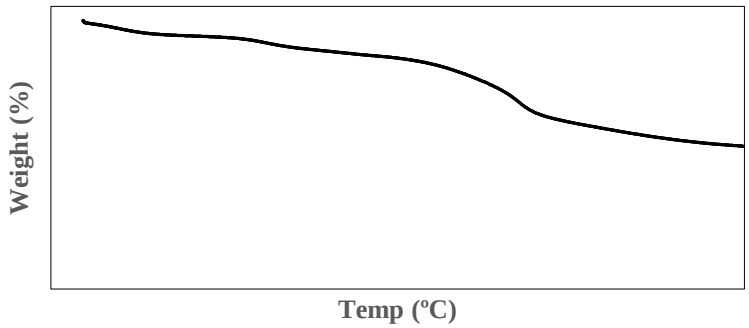

Figure 7: TGA graph of sample with core/wall=2.

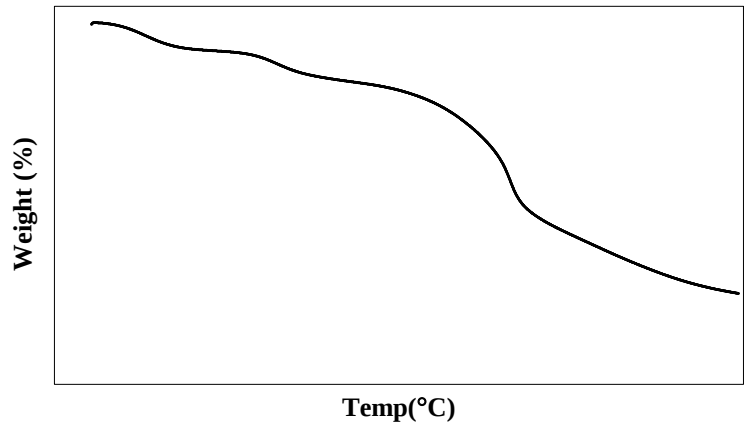

Figure 8: TGA graph of sample with core/wall=3.

Figure 9 demonstrates the significant influence of the core-to-wall ratio on encapsulation efficiency. As the ratio increased from 2:1 to 3:1, a corresponding decrease in encapsulation efficiency was observed, falling from 92 to 78 % (Mc2, Mc6). This inverse relationship can be attributed to two primary factors: first, the reduced availability of shell-forming precursors at higher core ratios limits complete interfacial polymerization, resulting in compromised microcapsule integrity. Second, thinner shell walls (as confirmed by TGA) exhibit greater susceptibility to mechanical damage during synthesis and isolation. These findings align with previous reports by Chen et al. [14] and Brown et al. [3], who reported similar efficiency reductions (15-20 %) when pushing core-to-wall ratios beyond optimal thresholds in melamine-formaldehyde systems. The results underscore the critical balance required between maximizing healing agent content and maintaining sufficient shell thickness for effective encapsulation.

3.5. Role of surfactant

a. On epoxy ring opening

White et al. developed an efficient encapsulation system using urea-formaldehyde (UF) resin, employing resorcinol and ammonium chloride as catalysts to enhance reactivity and encapsulation efficiency [4]. This method proved successful for dicyclopentadiene (DCPD) and various other core materials, yielding microcapsules with excellent morphological and mechanical properties. However, when applied to epoxy resin systems, the combination of ammonium chloride and low pH conditions was found to promote undesirable epoxy ring-opening reactions.

To address this limitation, subsequent studies explored alternative catalysts that could maintain the beneficial effects of ammonium chloride while preventing epoxy degradation. The introduction of Siquat BAC 80 as a surfactant proved particularly effective, as its quaternary ammonium groups localize preferentially at the epoxy/water interface without interacting with oxirane functionalities. This strategic modification achieves three critical objectives:

- Preservation of epoxy ring integrity
- Maintenance of high encapsulation efficiency

Effective interfacial catalysis comparable to ammonium chloride. The quaternary amino groups in Siquat BAC 80 remain confined to the droplet interface due to their amphiphilic nature, thereby preventing diffusion into the epoxy phase where they could initiate ring-opening reactions. This represents a significant advancement over conventional UF encapsulation methods when applied to epoxy-based healing agents.

b. On capsule morphology

Figures 10 a-c demonstrate the significant impact of surfactant concentration on microcapsule characteristics. Increasing the surfactant content from 1 to 5 % substantially improved size uniformity while simultaneously altering capsule morphology due to enhanced melamine-formaldehyde deposition at the interface. This effect arises from the surfactant's dual role in stabilizing the emulsion and catalyzing shell polymerization at the droplet surface.

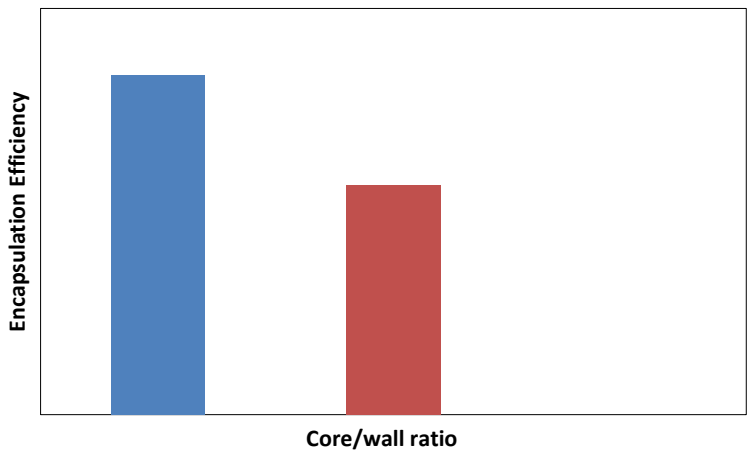

Figure 9: Encapsulation efficiency vs. core/wall ratio for Mc2 and Mc6.

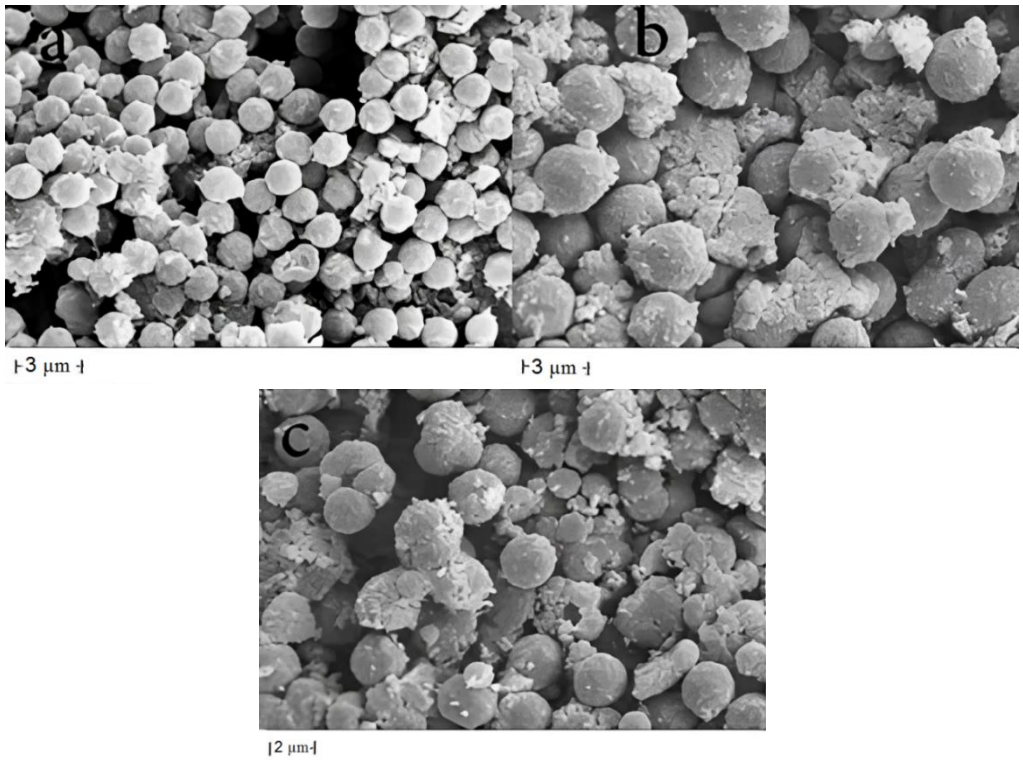

Figure 10: SEM images of samples synthesized with different amount of surfactant a) 1 %, b) 5 % and c) 10 %.

Further increasing the surfactant to 10 % led to two notable phenomena:

- Formation of irregular microcapsule aggregates through interparticle bridging
- Excessive precipitation of melamine-formaldehyde in the aqueous phase

These adverse effects result from surfactant saturation at the interface, where excess molecules migrate to the aqueous phase and catalyze uncontrolled polymerization. The optimal surfactant concentration was identified as 5 %, balancing spherical morphology preservation and minimal aqueous-phase precipitation.

c. On encapsulation efficiency

The necessity of maintaining an optimal surfactant concentration becomes evident when examining its profound impact on encapsulation efficiency. Figure 11 shows that excessive amounts (>1 wt. %) lead to a dramatic reduction in encapsulation efficiency (from 81 to 63 % at 10 wt. % surfactant). This efficiency decline stems from three primary mechanisms:

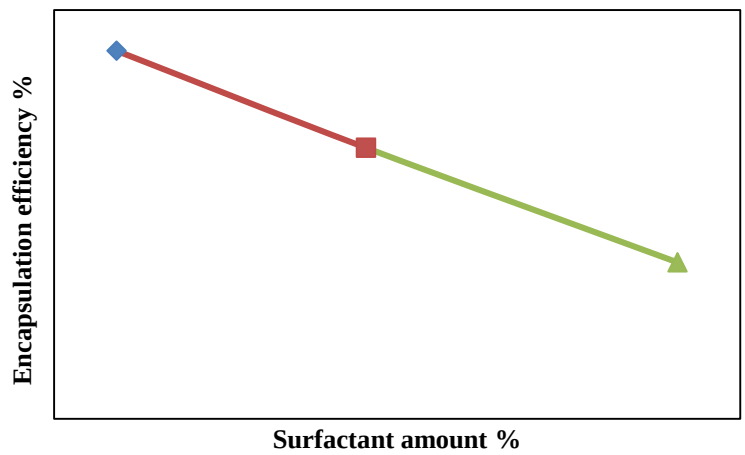

Figure 11: Encapsulation efficiency vs. surfactant amountfor Mc4, Mc8 and Mc7.

- Competitive micelle formation in the aqueous phase, which diverts shell precursors away from the oil-water interface
- Over-stabilization of droplets, inhibiting necessary coalescence for complete shell formation
- Uncontrolled homogeneous nucleation of melamine-formaldehyde in the bulk solution

The results in Table 1 show that in the optimum operational conditions, the sample Mc2 with 1 wt. % surfactant concentration emerged as the optimal balance, achieving 91.8 ± 2 % encapsulation efficiency. The sharp efficiency drop above 5 wt. % particularly highlights the delicate equilibrium required between interfacial stabilization and reaction kinetics in microencapsulation processes.

4. Conclusion

This study successfully developed a controlled, high-efficiency encapsulation system through systematic optimization of critical parameters. The implementation of Siquat BAC 80, a cationic surfactant featuring quaternary ammonium groups, proved transformative, achieving 92 % encapsulation efficiency while preserving core material integrity. This represents a significant advancement over conventional ammonium chloride-catalyzed systems, which compromise epoxy functionalities through ring-opening reactions. Two fundamental control mechanisms were established, including capsule diameter regulation via stirring rate modulation (500-1100 rpm), enabling precise size tuning from 2 to 1 μm while maintaining spherical morphology and interfacial stability optimization at 5 wt. % surfactant concentration. Contrary to theoretical predictions, excessive surfactant induced adverse effects, including irregular capsule aggregation and 28 % efficiency reduction at 10 wt. % surfactant, as well as homogeneous nucleation of melamine-formaldehyde nanoparticles. While this work establishes robust parameter control, further investigation should address reaction time, temperature, and pH optimization to suppress nanoparticle formation and shear-rate thresholds for different core viscosities. The developed methodology provides a versatile platform for microencapsulation, particularly valuable for self-healing composites requiring precise size-distribution and sensitive core materials vulnerable to traditional catalysts.

5. References

1. Blaiszik B, Kramer S, Olugebefola S, Moore J, Sottos N, White S. Self-Healing Polymers and Composites. Annu Rev Mater Res. 2010;40(1):179-211. https://doi.org/10.1146/annurev-matsci-070909-104532.
2. Zhang MQ, Rong MZ. Self-healing Polymers and Polymer Composites. John Wiley & Sons; 2011. ISBN: 978-0-470-49712-8.
3. Brown EN, Kessler MR, Sottos N.R , White SR. In situ poly(urea-formaldehyde) microencapsulation of dicyclopentadiene. J Microencapsul. 2003;20(6):719-730. https://doi.org/10.1080/0265204031000154160.
4. White SR, Sottos NR, Geubelle PH, Moore JS, Kessler MR, Sriram SR, et al. Autonomic healing of polymer composites. Nature. 2001;409(6822):794-7. https://doi.org/10.1038/35057232.
5. Wool RP. Self-healing materials: a review. Soft Mater. 2008; 4(3):400-18. https://doi.org/10.1039/B711716G.
6. Yuan YC, Yin T, Rong MZ, Zhang MQ. Self healing in polymers and polymer composites. concepts, realization and outlook: A review. Express Poly Lett. 2008;2(4): 238-250. https://doi.org/10.3144/expresspolymlett.2008.29.
7. Kessler MR. Self-healing: A new paradigm in materials design. Proceedings of the institution of mechanical engineers, Part G: J Aeros Eng. 2007;221(4):479-95. https://doi.org/10.1243/09544100JAERO172.
8. Caruso MM, Delafuente DA, Ho V, Sottos NR, Moore JS, White SR. Solvent-promoted self-healing epoxy taterials. Macromolecules. 2007;40(25):8830-2. https://doi.org/10.1021/MA701992Z.
9. Yang J, Keller MW, Moore JS, White SR, Sottos NR. Microencapsulation of Isocyanates for Self-Healing Polymers. Macromolecules. 2008;41(24):9650-9655. https://doi.org/10.1021/ma801718v.
10. Yao L, Yuan YC, Rong MZ, Zhang MQ. Self-healing linear polymers based on RAFT polymerization. Polymer. 2011;52(14):3137-45. https://doi.org/10.1016/j.polymer.2011.05.024.
11. Zhang C, Wang H, Zhou Q. Preparation and characterization of microcapsules based self-healing coatings containing epoxy ester as healing agent. Prog Org Coat. 2018;125:403-10. https://doi.org/10.1016/j.porgcoat. 2018.09.028
12. Safaei F, Khorasani SN, Rahnama H, Neisiany RE, Koochaki MS. Single microcapsules containing epoxy healing agent used for development in the fabrication of cost efficient self-healing epoxy coating. Prog Org Coat. 2018;114:40-6. https://doi.org/10.1016/j.porgcoat. 2017.09.019.

13. Altuna FI, Pettarin V, Williams RJJ. Self-healable polymer networks based on the cross-linking of epoxidised soybean oil by an aqueous citric acid solution. Green Chem. 2013;15(12):3360. https://doi.org/10.1039/C3GC41384E.
14. Chen PW, Cadisch G, Studart AR. Encapsulation of aliphatic amines using microfluidics. Langmuir. 2014; 30(9):2346-50. https://doi.org/10.1021/la500037d.
15. NguonO, Lagugné-Labarthet F, Brandys FA, Li J, Gillies ER. Microencapsulation byinsitu polymerization of amino resins. Poly Rev. 2018;58(2):326-375. https://doi.org/10.1080/15583724.2017.1364765.
16. Bolimowski PA, Bond IP, Wass DF. Robust synthesis of epoxy resin-filled microcapsules for application to self-healing materials. Phil Trans R Soc A. 2016;374 (2061):20150083.https://doi.org/10.1098/rsta.2015.0083.
17. Thakur T, Gaur B, Singha A. Bio-based epoxy/ imidoamine encapsulated microcapsules and their application for high performance self-healing coatings. Prog Org Coat. 2021;159:106436. https://doi.org/10. 1016/j.porgcoat.2021.106436.
18. Khorasani SN, Ataei S, Neisiany RE. Micro-encapsulation of a coconut oil-based alkyd resin into poly(melamine–urea–formaldehyde) as shell for self-healing purposes. Prog Org Coa. 2017; 111:99-106. https://doi.org/10.1016/j.porgcoat.2017.05.014.
19. Miyazaki N, Sugai Y, Sasaki K, Okamoto Y. Dual Role of citric acid as a binding inhibitor of anionic surfactant with bivalent cations and co-surfactant on bio-surfactant EOR. Abu Dhabi International Petroleum Exhibition & Conference. 2018. SPE-193277-MS. https://doi.org/10.2118/193277-MS
20. Zotiadis C, Patrikalos I, Loukaidou V, Korres DM, Karantonis A, Vouyiouka S. Self-healing coatings based on poly(urea-formaldehyde) microcapsules: In situ polymerization, capsule properties and application. Prog Org Coat. 2021;161:106475. https://doi.org/10. 1016/j.porgcoat.2021.106475.
21. Sharma S, Choudhary V. Poly(melamine-formaldehyde) microcapsules filled with epoxy resin: effect of M/F ratio on the shell wall stability. Mater Res Express. 2017;4(7):075307. https://doi.org/10.1088/2053-1591/aa7c8f.
22. Li W, Zhu X, Zhao N, Jiang Z. Preparation and properties of melamine urea-formaldehyde micro-capsules for self-healing of cementitious materials. Materials. 2016;9(3):152. https://doi.org/10.3390/ma9030152.
23. Ollier RP, Alvarez VA. Synthesis of epoxy-loaded poly(melamine-formaldehyde) microcapsules: Effect of pH regulation method and emulsifier selection. Colloids Surfaces A: Physicochem Eng Aspect. 2017; 520:872-82.http://dx.doi.org/doi:10.1016/j.colsurfa.2017.02.053.
24. Yu H, Zhang Y, Wang M, Li C. Dispersion of poly (urea-formaldehyde)-based microcapsules for self-healing and anticorrosion applications. Langmuir. 2019; 35(24):7871-8.https://doi.org/10.1021/acs.langmuir.9b00 526.
25. Jiang W, Zhou G, Wang C, Xue Y, Niu C. Synthesis and self-healing properties of composite microcapsule based on sodium alginate/melamine-phenol–formaldehyde resin. Const Building Mater. 2021; 271:121541. https://doi.org/10.1016/j.conbuildmat.2020.121541.
26. Parsaee S, Mirabedini SM, Farnood R, Alizadegan F. Development of self-healing coatings based on urea-formaldehyde/polyurethane microcapsules containing epoxy resin. J Appl Poly Sci. 2020;137(41): 49663. https://doi.org/10.1002/app.49663.
27. Tong X, Zhang T, Yang M, Zhang Q. Preparation and characterization of novel melamine modified poly (urea–formaldehyde) self-repairing microcapsules. Colloids Surf A: Physicochem Eng Aspects. 2010; 371(1-3):91-7. https://doi.org/10.1016/j.colsurfa.2010.09.009.
28. Zhang H, Wang R, Cheng F. Study on the properties and self-healing ability of asphalt and asphalt mixture containing methanol-modified melamine-formaldehyde microcapsules. Mater Today Commun. 2024;41:111007. https://doi.org/10.1016/j.mtcomm.2024.111007.
29. Dong B, Fang G, Ding W, Liu Y, Zhang J, Han N, et al. Self-healing features in cementitious material with urea–formaldehyde/epoxy microcapsules. Construction Building Mater. 2016; 106:608-17. https://doi.org/10.1016/j.conbuildmat.2015.12.140.

How to cite this article:
Babaei E, Pishvaei M, Najafi F. A Dual-Functional Surfactant Strategy for High-Yield Synthesis of Epoxy-Loaded Melamine Formaldehyde Microcapsules. Prog Color Colorants Coat. 2026;19(3): 363-373. https://doi.org/10.30509/pccc.2025.167621.1428.